Journal of Dental Research
2016, Vol. 95(4) 380–387
© International & American Associations for Dental Research 2015
Reprints and permissions:
sagepub.com/journalsPermissions.nav
DOI: 10.1177/0022034515623741
jdr.sagepub.com

Paucity of Nanolayering in Resin-Dentin Interfaces of MDP-based Adhesives

F. Tian[1*], L. Zhou[2*], Z. Zhang[3*], L. Niu[4], L. Zhang[1], C. Chen[5], J. Zhou[1], H. Yang[2], X. Wang[1], B. Fu[3], C. Huang[2], D.H. Pashley[6], and F.R. Tay[6]

Abstract

Self-assembled nanolayering structures have been reported in resin-dentin interfaces created by adhesives that contain 10-methacryloyloxydecyl dihydrogen phosphate (10-MDP). These structures have been hypothesized to contribute to bond durability. The objective of the present study was to determine the extent of nanolayering in resin-dentin interfaces after application of commercialized 10-MDP-containing self-etch and universal adhesives to human dentin. Seven commercialized adhesives were examined: Adhese Universal (Ivoclar-Vivadent), All-Bond Universal (Bisco, Inc.), Clearfil SE Bond 2, Clearfil S3 Bond Plus, Clearfil Universal Bond (all from Kuraray Noritake Dental Inc.), G-Premio Bond (GC Corp.), and Scotchbond Universal (3M ESPE). Each adhesive was applied in the self-etch mode on midcoronal dentin according to the respective manufacturer's instructions. Bonded specimens (n = 6) were covered with flowable resin composite, processed for transmission electron microscopy, and examined at 30 random sites without staining. Thin-film glancing angle X-ray diffraction (XRD) was used to detect the characteristic peaks exhibited by nanolayering (n = 4). The control consisted of 15%wt, 10%wt, and 5%wt 10-MDP (DM Healthcare Products, Inc.) dissolved in a mixed solvent (ethanol and water weight ratio 9:8, with photoinitiators). Experimental primers were applied to dentin for 20 s, covered with hydrophobic resin layer, and examined in the same manner. Profuse nanolayering with highly ordered periodicity (~3.7 nm wide) was observed adjacent to partially dissolved apatite crystallites in dentin treated with the 15% 10-MDP primer. Three peaks in the 2θ range of 2.40° (3.68 nm), 4.78° (1.85 nm), and 7.18° (1.23 nm) were identified from thin-film XRD. Reduction in the extent of nanolayering was observed in the 10% and 5% 10-MDP experimental primer-dentin interface along with lower intensity XRD peaks. Nanolayering and characteristic XRD peaks were rarely observed in specimens prepared from the commercialized adhesives. The sparsity of nanolayering in resin-dentin interfaces created by commercialized adhesives challenges its clinical effectiveness as a mechanism for improving bond longevity in dentin bonding.

Keywords: 10-MDP, transmission electron microscopy, x-ray diffraction, functional monomer, methacryloyloxydecyl dihydrogen phosphate, dental bonding

Introduction

The major problem encountered in dentin bonding is the limited durability of the clinical bonding outcomes (De Munck et al. 2005). The interface between resin and dentin is vulnerable to endogenous enzyme digestion, resin hydrolysis, and separation induced by mechanical stresses (Pashley et al. 2011; Van Meerbeek et al. 2011). Hence, the focus of contemporary dentin bonding research is to develop materials that promote long-term performance and bonding strategies that prevent degradation (Liu et al. 2011).

Chemical affinity between functional resin monomers and dentin has been investigated by X-ray diffraction (XRD), X-ray photoelectron spectroscopy, nuclear magnetic resonance (NMR), and Fourier transform-infrared spectroscopy. Results of these chemoanalytical analyses suggest that ionic bonding between some functional resin monomers and calcium ions may be stronger than the van der Waals forces and hydrogen bonds associated with micromechanical interlocking of collagen fibrils by polymerized resins (Yoshida et al. 2004; Fu et al. 2005; Fukegawa et al. 2006). To date, 10-methacryloyloxydecyl dihydrogen phosphate (MDP) is the most frequently reported functional resin monomer that bonds chemically to apatite crystallites (Yoshida et al. 2004). The ionic bond present in MDP-Ca salt was reported to be the most stable among

[1]Department of Cariology and Endodontology, Peking University School and Hospital of Stomatology, Beijing, PR China
[2]Key Laboratory for Oral Biomedical Ministry of Education, School & Hospital of Stomatology, Wuhan University, Wuhan, PR China
[3]Department of Prosthodontics, Zhejiang University School and Hospital of Stomatology, Hangzhou, China
[4]State Key Laboratory of Military Stomatology, School of Stomatology, The Fourth Military Hospital, Xi'an, Shaanxi, China
[5]Department of Operative Dentistry & Endodontics, Affiliated Hospital of Stomatology, Nanjing Medical University, Nanjing, PR China
[6]The Dental College of Georgia, Augusta University, Augusta, GA, USA
*Authors contributing equally to this article.

A supplemental appendix to this article is published electronically only at http://jdr.sagepub.com/supplemental.

Corresponding Authors:
F.R. Tay, The Dental College of Georgia, Augusta University, Augusta, GA, 30912-1129, USA.
Email: ftay@gru.edu
X. Wang, Department of Cariology and Endodontology, School and Hospital of Stomatology, Peking University, Beijing, China.
Email: wangxiaoyanpx@163.com

the functional monomers examined by Yoshihara et al. (2010). Nanolayered structures have been identified from transmission electron microscopy (TEM) images of 10-MDP-primed resin-dentin interfaces (Yoshihara et al. 2010; Yoshihara et al. 2011; Yoshida, Yoshihara, Nagaoka, et al. 2012; Yoshihara et al. 2013). According to those studies, the nanostructures represented self-assembled 10-MDP-Ca salts. Ultrastructural manifestation of 10-MDP-Ca nanolayering was corroborated with the demonstration of 3 characteristic peaks in the 2θ range of 2° to 8° in thin-film XRD scans of the adhesive-coated dentin (Yoshida, Yoshihara, Nagaoka, et al. 2012). In crystalline structures, peaks appearing at specific 2θ angles are associated with distances between periodic atomic structures. Thus, this finding was interpreted to be an indicator of chemical bonding. It has been hypothesized that nanolayering might be responsible for promoting the durability of resin-dentin bonds.

Because of the purported advantages of nanolayering in bonding to hard tooth structures and the chemical affinity of 10-MDP to zirconia, that phosphoric acid ester resin monomer has been included in many commercial self-etch and universal adhesives following expiration of the patents (Omura et al. 1985, 1987) owned by Kuraray Noritake Dental Inc. (Tokyo, Japan). In self-etch adhesive formulations, 2-hydroxyethyl methacrylate (HEMA) is commonly incorporated into adhesives to improve wetting of the dentin surface and to prevent phase separation of water-immiscible resin components after evaporation of the solvent. A recent study reported that 2-HEMA interfered with 10-MDP-Ca nanolayering formation; 10-MDP-Ca peaks in NMR and thin-film XRD were barely noticeable with incorporation of as little as 8% 2-HEMA to experimental MDP-HEMA formulations and using a hydroxyapatite interaction time of 5 min (Yoshida, Yoshihara, Hayakawa, et al. 2012). Paradoxically, some 2-HEMA-containing self-etch and universal adhesives have been shown to produce nanolayering structures under clinically relevant bonding conditions (Yoshida, Yoshihara, Nagaoka, et al. 2012; Yoshihara et al. 2013). These contradictory results create confusion regarding the nanolayering potential of 10-MDP in commercial dentin adhesives.

To enhance bond durability, 10-MDP-Ca nanolayering distribution should be ubiquitously identified, instead of being sporadically observed along the resin-dentin interface created by commercial 10-MDP-containing adhesives. Because these perplexing issues have not been adequately resolved in the literature, the objective of the present study was to determine the extent of nanolayering in resin-dentin interfaces after application of commercial 10-MDP-containing self-etch or universal adhesives to human dentin. The hypothesis tested was that 10-MDP-containing commercial adhesives are equally proficient in creating nanolayering in dentin compared with experimental 2-HEMA free 10-MDP primer formulations.

Materials and Methods

The present study used 102 noncarious human third molars. The use of human teeth for in vitro research was approved by the Human Assurance Committee of Georgia Regents University. The teeth were stored at 4 °C in 0.9% NaCl containing 0.02% sodium azide to prevent bacterial growth. A 2-mm-thick disk in coronal dentin was prepared from each tooth by making parallel cuts perpendicular to the longitudinal axis of the tooth, using a low-speed Isomet saw (Buehler Ltd., Lake Bluff, IL, USA) with water cooling. The dentin surface designated for bonding was polished with 600-grit silicon carbide paper under running water for 1 min to create a standardized smear layer. The dentin disks were randomly divided into 10 groups of 10 teeth each; the remaining 2 disks were used as mineralized dentin control.

To ensure that nanolayering could be identified in resin-dentin interfaces, 3 light-curable experimental primers containing different concentrations of 10-MDP as the exclusive resin component were prepared by mixing 10-MDP (DM Healthcare Products, Inc., San Diego, CA, USA), ethanol, and water at the ratios of 15:45:40 wt% (15% 10-MDP), 10:47.6:42.4 wt% (10% 10-MDP), and 5:50.3:44.7 wt% (5% 10-MDP), respectively. Camphorquinone (1 wt%) and ethyl-4-dimethylamino benzoate (0.4 wt%; both from Sigma-Aldrich, St. Louis, MO, USA) were subsequently added to the mixed solutions to render the primers light-curable (Musanje et al. 2009). The latter were protected from light and were refrigerated prior to use. The acidity of the experimental primers was determined with a pH meter (Orion Star A211, ThermoScientific, Waltham, MA, USA).

Seven 10-MDP-containing commercial adhesives were used for testing the first hypothesis: Adhese Universal (Ivoclar-Vivadent, Schaan, Liechtenstein); All-Bond Universal (Bisco, Inc. Schaumburg, IL, USA); Clearfil S3 Bond Plus, Clearfil SE Bond 2, Clearfil Universal Bond (all from Kuraray Noritake Dental Inc.); G-Premio Bond (GC Corp., Tokyo, Japan); and Scotchbond Universal (3M ESPE, St. Paul, MN, USA). Each adhesive was used in self-etch mode according to the respective manufacturer's instructions. Information on the composition and application procedures of these adhesives is provided in the Table.

Six teeth in each group were used for TEM of the resin-dentin interface. For the controls, each of the 3 experimental primers was applied to the surface of a dentin disk for 15 s with agitation. The primed dentin was air-dried for 5 s to remove water and the ethanol solvent and subsequently was light-cured for 20 s using a light-emitting diode light-curing unit (Valo, Ultradent, South Jordan, UT, USA). A layer of unfilled, 10-MDP-free resin (DE Bonding Resin, Bisco, Inc., Schaumburg, IL, USA) was applied to the primed dentin, air-thinned, and light-cured for 20 s. A 2-mm-thick layer of flowable resin composite (Clearfil Protect Liner F, Kuraray Noritake Dental Inc.) was applied over the bonded dentin and light-cured for 40 s. Bonding of each commercial adhesive was performed similarly by using the respective adhesive in the self-etching mode, according to the manufacturer's instructions.

After the specimens were stored in deionized water for 24 h, a 2-mm-thick strip was sectioned from the center of each composite-dentin disk and processed for TEM. Each nondemineralized strip was dehydrated in an ascending ethanol series (50% to 100%), immersed in propylene oxide as transition

Table. Commercially Available 10-MDP-Containing Adhesive Systems (in Alphabetical Order), Their Compositions, and Application Procedures (Self-Etch Technique).

Adhesive	Composition	Application (Self-Etching Mode)	pH	No. of Sites with Nanolayering[a]
Adhese Universal (Ivoclar-Vivadent, Schaan, Liechtenstein)	10-MDP, 2-HEMA, Bis-GMA, MCAP, D3MA, highly dispersed silica, ethanol, water, photoinitiators	1. Scrub 1 coat of adhesive for 20 s. 2. Gently air-thin until a glossy, immobile film layer results. 3. Light-cure for 10 s.	2.5–3.0	0
All-Bond Universal (Bisco, Inc., Schaumburg, IL, USA)	10-MDP, 2-HEMA, Bis-GMA, ethanol, water, photoinitiators	1. Apply 2 separate coats of adhesive, scrubbing with microbrush for 10–15 s per coat. 2. Evaporate excess solvent by thoroughly air-drying with an air syringe for at least 10 s until achieving a uniform glossy appearance. 3. Light-cure for 10 s.	3.2	0
Clearfil S3 Bond Plus (Kuraray Noritake Dental Inc., Tokyo, Japan)	10-MDP, 2-HEMA, Bis-GMA, hydrophilic and hydrophobic aliphatic dimethacrylates, sodium fluoride, colloidal silica, ethanol, water, photoinitiators	1. Apply bond and leave undisturbed for 10 s. 2. Dry by blowing mild air for more than 5 s until the bond does not move. 3. Light-cure for 10 s.	2.7	2
Clearfil SE Bond 2 (Kuraray Noritake Dental Inc., Tokyo, Japan)	*Primer*: 10-MDP, 2-HEMA, hydrophilic dimethacrylate, water, photoinitiator *Bond*: 10-MDP, 2-HEMA, Bis-GMA, hydrophobic dimethacrylate, silanized colloidal silica, photoinitiators	1. Apply primer and leave undisturbed for 20 s. 2. Dry by blowing mild air for more than 5 s. 3. Apply bond and make the resin film as uniform as possible using gentle oil-free air-stream. 4. Light-cure for 10 s.	2.0	5
Clearfil Universal Bond (Kuraray Noritake Dental Inc., Tokyo, Japan)	10-MDP, 2-HEMA, Bis-GMA, hydrophilic aliphatic dimethacrylate, silane coupling agent, colloidal silica, photoinitiators	1. Apply bond and rub for 10 s. 2. Dry by blowing mild air for more than 5 s until the bond does not move. 3. Light-cure for 10 s.	2.3	0
G-Premio Bond (GC Corp., Tokyo, Japan)	10-MDP, 4-META, 10-methacryloyloxydecyl dihydrogen thiophosphate, methacrylic acid ester, acetone, water, photoinitiators	1. Apply adhesive (0 s no waiting option used in the present study); can be left untouched for up to 10 s. 2. Dry by blowing air for 5 s. 3. Light-cure for 5 s.	1.4–1.8	0
Scotchbond Universal (3M ESPE, St. Paul, MN, USA)	10-MDP, 2-HEMA, silane, dimethacrylate resins, methacrylate modified polyalkenoic acid copolymer, filler, ethanol, water, photoinitiators	1. Apply the adhesive to the entire preparation and agitate for 20 s. 2. Gently air-blow over the liquid for 5 s until the latter no longer moves. 3. Light-cure for 10 s.	2.7	0

2-HEMA, 2-hydroxyethyl methacrylate; 4-META, 4-methacryloyloxyethy trimellitate anhydride; 10-MDP, 10-methacryloyloxydecyl dihydrogen phosphate; Bis-GMA, bisphenol A glycidyl methacrylate; D3MA, decandiol dimethacrylate; MCAP, methacrylated carboxylic acid polymer.
[a]Out of 30 random sites (5 locations per section × 6 sections).

medium, and embedded in epoxy resin. Ninety-nanometer-thick sections ($n = 6$; 1.5 mm × 1.5 mm each) were prepared using an ultramicrotome. The sections were examined without staining using a JEM-1230 TEM (JEOL, Tokyo, Japan) at 110 kV. One thin section was obtained from each tooth and loaded onto 1 TEM grid ($n = 6$). Each thin section derived from 1 tooth was examined at 5 randomly selected sites along the resin-dentin interface for the presence or absence of nanolayering. For 6 teeth, this yielded 6 teeth × 5 sites per tooth = 30 examination sites for each primer/adhesive.

Equal amounts of 0.005 mol/L 10-MDP in ethanol (with photoinitiator) and $CaCl_2$ of the same molar concentration in water were mixed on a polymerized polymethyl methacrylate resin surface. After solvent evaporation, the deposited monomer-calcium salts were light-polymerized and processed for TEM observation as described above. This served as a control for nanolayering formation on a nondental surface.

The remaining 4 teeth from each group were used for thin-film XRD. The experimental primer, the primer of 2-step self-etch commercial adhesive, or the commercial universal adhesive was applied to a dentin surface for the designated time, air-dried to remove solvents, and left uncured. Each specimen was subjected to thin-film glancing angle XRD (CuKα XRD; d/max2500, Rigaku, Tokyo, Japan) at 40 kV and 200 mA. Because X-ray penetration depth in thin films is a function of the incident beam angle (Kobayashi, 2010), the latter was kept low and fixed at 1.0° to maximize the detection of diffraction peaks associated with the formation of nanolayered 10-MDP-Ca salts. This helped to avoid intense signals derived from the underlying dentin substrate and generate stronger signals from the adhesive film. A scanning time of 0.02°/s was used for 2θ scan from 0.6° to 40°. The 2 untreated mineralized dentin disks were used to generate XRD patterns of carbonated apatite present in the dentin substrate.

Results

The pH values of 10-MDP experimental primer solutions were 2.62, 2.64, and 2.65 for the 5%, 10%, and 15% solutions, respectively. Profuse nanolayering was observed along the resin-dentin interface of 15% 10-MDP primer–treated specimens (30 of 30 random sites; Fig. 1A–C). Nanolayering was identified within an amorphous layer on top of the hybrid layer. These nanostructures were arranged in 12 to 15 parallel layers into 3-dimensional arrays (Fig. 1D), some of which were associated with remnant apatite crystallites. The nanolayer thickness ($n = 100$) measured by image analysis (Image J, National Institutes of Health, Bethesda, MD, USA) was 3.70 ± 0.31 nm. Thin-film glancing angle XRD of 15% experimental primer–treated dentin showed 3 strong peaks at 2.40°, 4.78°, and 7.18° 2θ (Fig. 1E, F). The calculated d-spacing based on the peak with the strongest signal was 3.68 nm, which is close to the nanolayer thickness measured by image analysis. These peaks were absent from the XRD spectrum of untreated dentin (Fig. 1E, F). Similar nanolayering features were also identified from the deposited monomer-calcium salt on the control polymethyl methacrylate resin surface (not shown).

Nanolayering was identified without difficulty from TEM images of 10% and 5% 10-MDP primer–treated dentin (30 out of 30 random sites for both experimental primers). Nanolayering became sparser with reduction in 10-MDP concentrations (Appendix

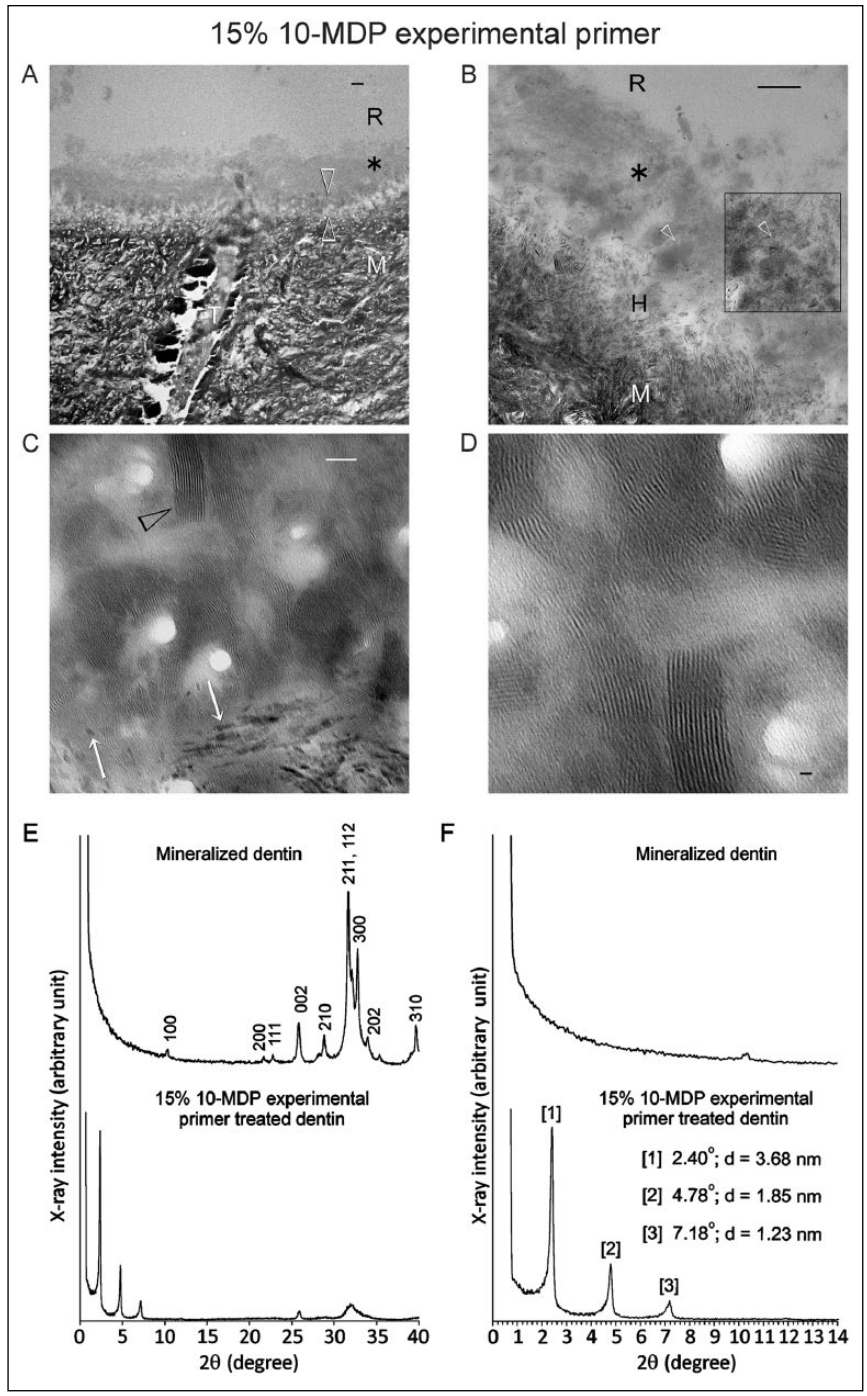

Figure 1. Application of 15% 10-methacryloyloxydecyl dihydrogen phosphate (10-MDP) experimental primer with no additional resinous components (pH 2.65) to coronal dentin in the self-etching mode, showing profuse nanolayering in the resin-dentin interface. (**A–D**) Transmission electron microscopy (TEM) images of unstained, nondemineralized sections of the resin-dentin interface. (A) A layer of gray mineral salt deposits (asterisk) formed by the interaction between the acidic resin monomer and dissolved calcium and phosphate ions is present on top of the 0.5- to 1-µm-thick hybrid layer (between open arrowheads). Bar = 500 nm. (B) Partially demineralized apatite crystallites are present within the hybrid layer (H). Nanolayering is profusely observed within the mineral salt layer (open arrowheads) particularly after contrast enhancement (box). Bar = 200 nm. (C) Extensive nanolayering (arrowhead) is present within the mineral salt layer (no contrast enhancement). Some of the electron-dense nanolayers were associated with remnant apatite crystallites (white arrows) in the hybrid layer. Bar = 50 nm. (D) Nanolayers are arranged in 12 to 15 parallel layers into discrete 3-dimensional arrays (no contrast enhancement). Bar = 10 nm.

(**E**) Thin-film glancing angle X-ray diffraction (XRD) spectra of untreated mineralized dentin (top) and dentin after self-etching with the experimental 10-MDP primer (bottom). Miller (*hkl*) indices of diffraction peaks characteristic of hydroxyapatite, depicted for untreated dentin, are also identified from the primer-treated dentin. (**F**) High magnification of Figure 1E in the 2° to 14° 2θ range. The 3 diffraction peaks (with corresponding reflection angles and calculated interatomic (d) spacings) present in the 15% 10-MDP-treated dentin are indicative of short-range order in the 10-MDP-Ca salts. These peaks are absent in the XRD spectrum of untreated dentin. R, adhesive resin; M, mineralized dentin; T, dentinal tubule.

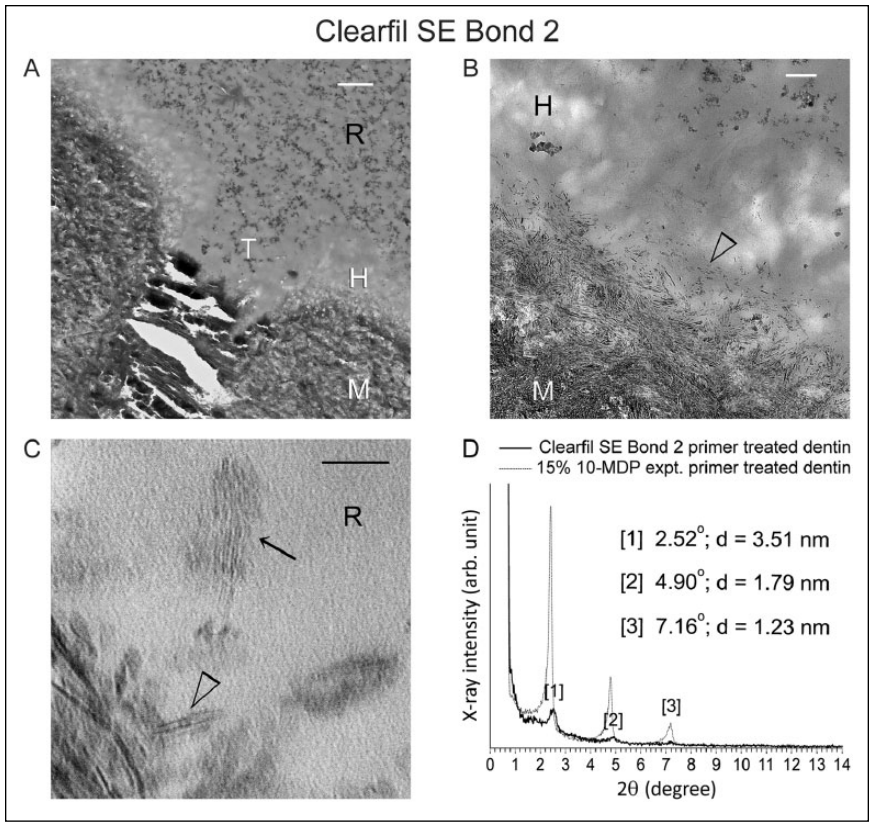

Figure 2. Resin-dentin interface created by a commercial adhesive that contains 10-methacryloyloxydecyl dihydrogen phosphate (10-MDP) (Clearfil SE Bond 2; pH 2.0 for primer) in coronal dentin, in which limited nanolayering was occasionally identified. (**A**) Transmission electron microscopy (TEM) image taken from an unstained, nondemineralized section. Bar = 500 nm. (**B**) Partially demineralized apatite crystallites (open arrowhead) are present within the hybrid layer. Bar = 200 nm. (**C**) Representative example of the sparse nanolayering identified in 1 of the sections (black arrow). Arrowhead: remnant apatite crystallites within the hybrid layer. Bar = 50 nm. (**D**) Thin-film glancing angle X-ray diffraction (XRD) spectrum from 2° to 14° 2θ, created by the application of Clearfil SE Bond 2 primer on dentin (solid line). Three small peaks derived from 10-MDP-Ca salts are visible, with their corresponding reflection angles and calculated d-spacings. For comparison, the diffraction profile of 15% 10-MDP experimental primer–treated dentin (dotted line) was superimposed over that created by Clearfil SE Bond 2 using the same horizontal and vertical scales. Without using Rietveld refinement, the empirical ratio of the first diffraction peak (lowest 2θ) of Clearfil SE Bond 2 primer–treated dentin to the 15% 10-MDP primer–treated dentin was estimated to be 0.164. R, filled adhesive resin; T, dentinal tubule; M, mineralized dentin; H, hybrid layer.

Figs. 1 and 2, A–C) when compared with the 15% 10-MDP-treated specimens. Thin-film glancing angle XRD results indicated that the peaks for 10% 10- MDP-treated specimens were located at 2.50°, 4.84°, and 7.18° 2θ, and those for 5% 10-MDP-treated dentin were located at 2.45°, 4.80°, and 7.18° 2θ. The measured nanolayer thickness was 3.51 ± 0.43 nm compared with the calculated d-spacing of 3.53 nm for the 10% 10-MDP primer and was 3.60 ± 0.38 nm compared with calculated d-spacing of 3.61 nm for the 5% 10-MDP primer–treated specimens. The intensity of the characteristic peaks of 10-MDP-Ca salt also reduced as 10-MDP concentration decreased (Appendix Figs. 1D and 2D); without additional Rietveld refinement, the empirical ratio of the strongest peak between 2.4° and 2.5° 2θ for the 15%, 10%, and 5% 10-MDP primers was 1:0.339: 0.234.

The number of random sites from which nanolayering could be identified by the 7 adhesives is summarized in the Table. Nanolayering could only be identified from limited sites in resin-dentin interfaces created by Clearfil SE Bond 2 (Fig. 2) and Clearfil S3 Bond Plus (Appendix Fig. 3). Ultrastructural images of Clearfil SE Bond 2 showed not only limited nanolayering but also less well-organized patterns compared with those formed by the pure 10-MDP primer (Fig. 2, A–C). Weak diffraction peaks associated with 10-MDP-Ca salt were present in the thin film glancing angle XRD scans, located at 2.52°, 4.70°, and 7.16° 2θ (ratio of first diffraction peak against that of the 15% experimental primer = 0.164). For Clearfil S3 Bond, even sparser nanolayering could be identified (Appendix Fig. 3, A–C) corroborating with the XRD result showing very weak peaks associated with the 10-MDP-Ca salt (ratio of first diffraction peak against that of the 15% experimental primer = 0.050).

Nanolayering could not be identified from any of the 30 random sites in resin-dentin interfaces created by the rest of the commercial adhesives. A representative example (Scotchbond Universal) is illustrated in Figure 3. Data for Adhese Universal, All-Bond Universal, Clearfil Universal Bond, and G-Premio Bond are included in Appendix Figures 4, 5 6, and 7, respectively. As representatively illustrated by the TEM images derived from Scotchbond Universal–treated dentin (Fig. 3, A–C), no nanolayering could be identified despite the formation of amorphous salt-like aggregates around the partially dissolved apatite crystallites within and on top of the hybrid layer. From the thin-film glancing angle XRD scan (Fig. 3D), characteristic peaks of 10-MDP-Ca salt were absent in the respective 2θ range (Fig. 3).

Discussion

The results of the present study do not allow us to validate the hypothesis that 10-MDP-containing commercial adhesives are equally proficient in creating nanolayering in dentin compared with experimental 2-HEMA-free 10-MDP primer formulations. The sparsity of nanolayering in resin-dentin interfaces created by the commercial adhesives probably resulted from the high percentages of 2-HEMA in their compositions (with

the exception of G-Premio Bond, which contains no 2-HEMA; Table). It has been reported that 2-HEMA interferes with 10-MDP-Ca nanolayering; 10-MDP-Ca peaks in NMR and thin-film XRD were barely noticeable with incorporation of as little as 8% 2-HEMA into experimental MDP-HEMA formulations with a hydroxyapatite interaction time of 5 min (Yoshida, Yoshihara, Hayakawa, et al. 2012). Others have reported that nanolayering is influenced by factors including 10-MDP concentration, adhesive agitation during application, purity of the 10-MDP, and the structure of functional monomers used in the adhesive (Yoshihara et al. 2011; Yoshihara et al. 2013). In the present study, although the 10-MDP synthesized by DM Healthcare Products is not as pure as the version manufactured by Kuraray Noritake Dental Inc. under active patent protection (Okada et al. 2002), even the 5% 10-MDP experimental primer produced far more nanolayering than did those 10-MDP-containing adhesives that exhibited nanolayering (Clearfil SE Bond 2 and Clearfil S3 Bond Plus). The nanolayering features produced by the 10-MDP used in the present study were nearly the same with previous results produced using the Kuraray 10-MDP source (Yoshihara et al. 2011; Yoshihara et al. 2013).

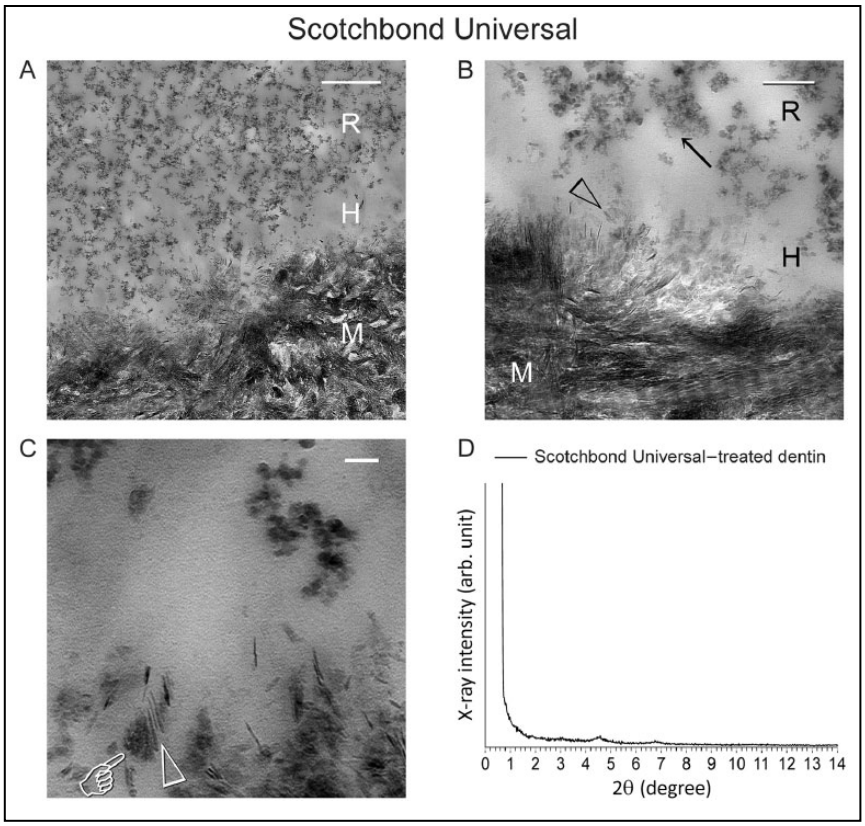

Figure 3. Representative example of resin-dentin interface created by a commercial adhesive that contains 10-methacryloyloxydecyl dihydrogen phosphate (10-MDP) (Scotchbond Universal; pH 2.7) in coronal dentin, in which no nanolayering could be identified in any location or section. (**A**) Low-magnification transmission electron microscopy (TEM) image taken from an unstained, nondemineralized section. A 0.5-µm-thick hybrid layer (H) is present between the filled adhesive resin (R) and mineralized dentin (M). Bar = 500 nm. (**B**) Remnant apatite crystallites (open arrowhead) are present within the hybrid layer (H). Nano-sized filler clusters (arrow) can be found in adhesive resin (R). Bar = 200 nm. (**C**) High-magnification image showing formation of mineral salts (pointer) around remnant apatite crystallites (open arrowhead), with no evidence of nanolayering. Bar = 50 nm. (**D**) Thin-film glancing angle X-ray diffraction (XRD) spectrum from 2° to 14° 2θ of Scotchbond Universal–treated dentin. The scan was plotted using the same horizontal and vertical scales as Figure 2D. Characteristic peaks of 10-MDP-calcium salt can barely be discerned. M, mineralized dentin.

Because nanolayering was so infrequently identified from resin-dentin interfaces created by commercial 10-MDP-containing adhesives, it is not unreasonable to challenge whether nanolayering by 10-MDP-Ca salts can really protect the adhesive interface from degradation in clinical scenarios. The hypothesized benefits of nanolayering include protecting collagen fibrils from water-induced degradation because of their hydrophobicity, increasing the resistance of residual apatite crystallites to acidic dissolution, and creating a more gradual transition between the inorganic bonding substrate and the biomaterial. While these assumptions await experimental validation, the direct contribution of chemical bonding to the overall bonding performance remains ambiguous.

Nanolayering has been postulated to be a self-assembly process of 10-MDP (Fukegawa et al. 2006), with the 10-MDP molecule acting as a surfactant in dentin adhesive formulations. Because of their amphiphilic properties, surfactant molecules exhibit a tendency to aggregate, with the hydrophilic domains exposed to water and the hydrophobic domains shielded from water (Hill et al. 2014). In aqueous solutions, surfactant molecules and amphiphiles self-assemble into various microstructures such as micelles, monolayer or bilayer, column-shaped, or cubic mesophases (Hao and Hoffman 2004; Ramanathan et al. 2013). Deposition of amorphous minerals by sol-gel reactions over these self-assembled 2D or 3D surfactant or amphiphile templates produces mesoporous materials with highly ordered hollow architecture after removal of the surfactants, the periodicity of which may be identified by small-angle XRD (Li and Shi 2014). A well-known example is mesoporous silica (Li et al. 2012); different types of amorphous mesoporous silica exhibit several small-angle XRD peaks that are characteristic of their internal porous architecture (Kruk et al. 1999, 2000; Solovyov et al. 2005). Crystalline solids possess both long-range and short-range order; the former is characterized by well-defined, strong intensity Bragg peaks when examined by XRD. Once the positions of an atom and its neighbors are known at one point, the positions of other atoms can be identified precisely in 3 dimensions throughout the crystal. In contrast, amorphous solids do not possess long-range order. The positions of the

first-neighbor atoms are predictable; however, the positions of atoms at a faraway distance become uncorrelated. Thus, discrete, sharp Bragg peaks are absent from the XRD spectrum (Bicerano and Alder 1987). For quasi-crystalline analogs of amorphous solids such as mesoporous silica, small-angle diffraction peaks arise from the highly ordered distances within the closely approximated nanochannel systems, rather than from regular atomic repeat distances (Edler 1997). This means that the nanolayering structure of 10-MDP-Ca salts possesses short-range order but lacks long-range order that is the hallmark of crystalline solids. Hence, the 3 peaks in the low 2θ range exhibited by nanolayering of 10-MDP-Ca salts are simply phenomenological manifestations of mesoporosity produced by highly ordered, porous amorphous solids. These peaks should not be misinterpreted as evidence of chemical bonding between 10-MDP-Ca salts and apatite. Both XPS and solid-state NMR evidence should demonstrate the presence of new peaks before one can determine whether chemical bonding is really present.

Theoretically, absence of 2-HEMA in G-Premio Bond favors nanolayering formation. However, acetone in the composition may influence nanolayering formation through changing polarity of the solvent and thereafter the hydrophobic effect of MDP molecule in the solution (Michor and Berg 2014). The adhesive also contains 4-methacryloyloxyethy trimellitate anhydride (4-META), which hydrolyzes into 4-MET on contact with water. There were no corresponding Bragg peaks associated with 4-MET-Ca salts when the carboxyl functional monomer was applied on the surface of apatite (Yoshihara et al. 2010). According to the packing parameter concept (Israelachvili et al. 1976), the aromatic headgroup of 4-MET results in larger equilibrium area per molecule at the aggregate interface, which hinders formation of micelle lamellae. A similar effect could have adversely restricted nanolayering formation by 10-MDP-Ca salts when 4-MET is present in adhesive formulations. In self-etch adhesive formulations, many components are blended together, including functional resin monomer, cross-linking resin monomers, solvents, fillers, and initiator systems (Moszner et al. 2005). These components further increase the complexity of the self-assembly environment.

Being amorphous structures with short-range order, the 10-MDP-Ca salts are formed by initial adsorption of the ionized 10-MDP molecules onto the hydrophilic dentin surface via electrostatic attraction. This is subsequently strengthened by the strong chemical bonding potential of 10-MDP-Ca salts (Yoshida et al. 2004; Yoshida and Inoue 2012). The layered 10-MDP molecules are further strengthened by polymerization of the neighboring C=C bond, which increases the robustness of nanolayers and makes the electron-dense calcium salt layers easier to observe under high-magnification TEM (Lee et al. 2009). Although stronger than surfactant micelles, the weak link in the nanolayering-adhesive interface is the poor cross-linking capability of 10-MDP molecules compared with cross-linking dimethacrylates. This probably limits the long-term stability of 10-MDP-Ca salts. Moreover, the 10-MDP-Ca ionic bond that is located in the hydrophilic domain of the amorphous salt may hydrolyze slowly with time, especially in acidic environments and under carious challenge. This may explain why nanolayering has never been observed by TEM in the completely demineralized specimens.

In conclusion, nanolayering is a rare finding in resin-dentin interfaces created by commercial 10-MDP-containing self-etch and universal adhesives. This nanoscale morphological feature represents self-assembled short-range order seen in amorphous solids and has conceptual rather than practical implications. The long-term stability of nanolayering as well as its potential impact on the macro-scale bonding behavior should be substantiated by evidence in future studies before any inferences are made regarding 10-MDP-Ca salt nanolayering and bond stability.

Author Contributions

F. Tian, L. Zhou, contributed to design, data acquisition, analysis, and interpretation, drafted the manuscript; Z. Zhang, contributed to design, data acquisition, and analysis, drafted the manuscript; L. Niu, F.R. Tay, contributed to conception, design, data acquisition, analysis, and interpretation, critically revised the manuscript; L. Zhang, C. Chen, contributed to data acquisition, drafted the manuscript; J. Zhou, X. Wang, B. Fu, contributed to data acquisition and interpretation, drafted the manuscript; H. Yang, C. Huang, contributed to data analysis and interpretation, drafted the manuscript; D.H. Pashley, contributed to conception, design, and data interpretation, critically revised the manuscript. All authors gave final approval and agree to be accountable for all aspects of the work.

Acknowledgments

This work was supported by grant R01 DE015306-06 from the National Institute of Dental and Craniofacial Research (D.H. Pashley); grant 2015AA020942 from National High Technology Research and Development Program of China, grant 81400555 from NSFC, and program IRT13051 from PCSIRT (L. Niu); and grant Z14110000514016 from Beijing Municipal Science & Technology Commission Project (X. Wang). The authors declare no potential conflicts of interest with respect to the authorship and/or publication of this article.

References

Bicerano J, Adler D. 1987. Theory of the structures of non-crystalline solids. Pure Appl Chem. 59(1):101–144.

De Munck J, Van Landuyt K, Peumans M, Poitevin A, Lambrechts P, Braem M, Van Meerbeek B. 2005. A critical review of the durability of adhesion to tooth tissue: methods and results. J Dent Res. 84(2):118–132.

Edler KJ. 1997. Template induction of supramolecular structure: synthesis and characterization of the mesopore molecular sieve, MCM-41 [dissertation]. Canberra (Australia): The Australian National University. p. 65–134.

Fu B, Sun X, Qian W, Shen Y, Chen R, Hannig M. 2005. Evidence of chemical bonding to hydroxyapatite by phosphoric acid esters. Biomaterials. 26(25):5104–5110.

Fukegawa D, Hayakawa S, Yoshida Y, Suzuki K, Osaka A, Van Meerbeek B. 2006. Chemical interaction of phosphoric acid ester with hydroxyapatite. J Dent Res. 85(10):941–944.

Hao J, Hoffmann H. 2004. Self-assembled structures in excess and salt-free cationic surfactant solutions. Curr Opin Colloid Interface Sci. 9(3–4):279–293.

Hill JP, Shrestha LK, Ishihara S, Ji Q, Ariga K. 2014. Self-assembly: from amphiphiles to chromophores and beyond. Molecules. 19(6):8589–8609.

Israelachvili JN, Mitchell DJ, Ninham BW. 1976. Theory of self-assembly of hydrocarbon amphiphiles into micelles and bilayers. J Chem Soc, Faraday Trans 2. 72:1525–1568.

Kobayashi S. 2010. X-ray thin-film measurement techniques. IV. In-plane CRD measurements. Rigaku J. 26(1):3–11.

Kruk M, Jaroniec M, Kim JM, Ryoo R. 1999. Characterization of highly ordered MCM-41 silicas using X-ray diffraction and nitrogen adsorption. Langmuir. 15(16):5279–5284.

Kruk M, Jaroniec M, Kim JM, Ryoo R. 2000. Characterization of the porous structure of SBA-15. Chem Mater. 12(7):1961–1968.

Lee JH, Danino D, Raghavan SR. 2009. Polymerizable vesicles based on a single-tailed fatty acid surfactant: a simple route to robust nanocontainers. Langmuir. 25(3):1566–1571.

Li Y, Shi J. 2014. Hollow-structured mesoporous materials: chemical synthesis, functionalization and applications. Adv Mater. 26(20):3176–3205.

Li Z, Barnes JC, Bosoy A, Stoddart JF, Zink JI. 2012. Mesoporous silica nanoparticles in biomedical applications. Chem Soc Rev. 41(7):2590–2205.

Liu Y, Tjäderhane L, Breschi L, Mazzoni A, Li N, Mao J, Pashley DH, Tay FR. 2011. Limitations in bonding to dentin and experimental strategies to prevent bond degradation. J Dent Res. 90(8):953–968.

Michor EL, Berg JC. 2014. Micellization behavior of aerosol OT in alcohol/water systems. Langmuir. 30(42):12520–12524.

Moszner N, Salz U, Zimmermann J. 2005. Chemical aspects of self-etching enamel-dentin adhesives: a systematic review. Dent Mater. 21(10):895–910.

Musanje L, Ferracane JL, Sakaguchi RL. 2009. Determination of the optimal photoinitiator concentration in dental composites based on essential material properties. Dent Mater. 25(8):994–1000.

Okada K, Otsuki J, Takahashi K, Minami Y, Terakawa E, Harada M, inventors; Kuraray Co., Ltd., assignee. 2002 Sep 3. Organophosphorus compounds for dental polymerisable compositions. United States patent US 6,458,868.

Omura I, Yamauchi J, Nagase Y, Uemura F, inventors; Kuraray Co., Ltd., assignee. 1985 Sep 3. Adhesive composition. United States patent US 4,539,382.

Omura I, Yamauchi J, Nagase Y, Uemura F, inventors; Kuraray Co., Ltd., assignee. 1987 Mar 17. Adhesive composition. United States patent US 4,650,847.

Pashley DH, Tay FR, Breschi L, Tjäderhane L, Carvalho RM, Carrilho M, Tezvergil-Mutluay A. 2011. State of the art etch-and-rinse adhesives. Dent Mater. 27(1):1–16.

Ramanathan M, Shrestha LK, Mori T, Ji Q, Hill JP, Ariga K. 2013. Amphiphile nanoarchitectonics: from basic physical chemistry to advanced applications. Phys Chem Chem Phys. 15(26):10560–10611.

Solovyov LA, Belousov OV, Dinnebier RE, Shmakov AN, Kirik SD. 2005. X-ray diffraction structure analysis of MCM-48 mesoporous silica. J Phys Chem B. 109(8):3233–3237.

Van Meerbeek B, Yoshihara K, Yoshida Y, Mine A, De Munck J, Van Landuyt KL. 2011. State of the art of self-etch adhesives. Dent Mater. 27(1):17–28.

Yoshida Y, Nagakane K, Fukuda R, Nakayama Y, Okazaki M, Shintani H, Inoue S, Tagawa Y, Suzuki K, De Munck J, et al. 2004. Comparative study on adhesive performance of functional monomers. J Dent Res 83(6):454–458.

Yoshida Y, Inoue S. 2012. Chemical analyses in dental adhesive technology. Jap Dent Sci Rev. 48(2):141–152.

Yoshida Y, Yoshihara K, Nagaoka N, Hayakawa S, Torii Y, Ogawa T, Osaka A, Meerbeek BV. 2012. Self-assembled nano-layering at the adhesive interface. J Dent Res. 91(4):376–381.

Yoshida Y, Yoshihara K, Hayakawa S, Nagaoka N, Okihara T, Matsumoto T, Minagi S, Osaka A, Van Landuyt K, Van Meerbeek B. 2012. HEMA inhibits interfacial nano-layering of the functional monomer MDP. J Dent Res. 91(11):1060–1065.

Yoshihara K, Yoshida Y, Nagaoka N, Fukegawa D, Hayakawa S, Mine A, Nakamura M, Minagi S, Osaka A, Suzuki K, et al. 2010. Nano-controlled molecular interaction at adhesive interfaces for hard tissue reconstruction. Acta Biomater. 6(9):3573–3582.

Yoshihara K, Yoshida Y, Hayakawa S, Nagaoka N, Irie M, Ogawa T, Van Landuyt KL, Osaka A, Suzuki K, Minagi S, et al. 2011. Nanolayering of phosphoric acid ester monomer on enamel and dentin. Acta Biomater. 7(8):3187–3195.

Yoshihara K, Yoshida Y, Nagaoka N, Hayakawa S, Okihara T, De Munck J, Maruo Y, Nishigawa G, Minagi S, Osaka A, et al. 2013. Adhesive interfacial interaction affected by different carbon-chain monomers. Dent Mater. 29(8):888–897.